Letter

Editors' Suggestion

Lateral flow interactions enhance speed and stabilize formations of flapping swimmers

Joel W. Newbolt, ^{1,2} Jun Zhang, ^{1,2,3,*} and Leif Ristroph ^{1,†}

¹Applied Mathematics Laboratory, Courant Institute, New York University, New York, New York 10012, USA

²Department of Physics, New York University, New York, New York 10003, USA

³NYU-ECNU Institutes of Physics and Mathematics at NYU Shanghai, Shanghai, China



(Received 9 April 2021; accepted 15 April 2022; published 6 June 2022)

While classic hydrodynamic models predict ordered formations for fish schools, observations show that schools are seemingly disordered. Our experiments on robotic swimmers may help to reconcile this discrepancy by showing that many different formations all emerge spontaneously and are stabilized due to flow interactions. Surprisingly, these locked states extend almost twice as far downstream for laterally displaced swimmers as for those in line. We also observe significant boosts in swimming speed—up to 60% faster than an isolated swimmer—for side-by-side formations. These findings demonstrate that benefits such as group cohesion and speed enhancement arise naturally via flow interactions and for the diverse relative arrangements seen in schools.

DOI: 10.1103/PhysRevFluids.7.L061101

Introduction. Fluid flows are an essential but unseen factor in many forms of group locomotion, from swarms of swimming bacteria [1] or flying insects [2] to bird flocks and formations [3,4] and fish schools [5-8]. Schooling exemplifies collective motion in biology and physics, but the role of flows as mediators of the physical interactions between swimming fish remains poorly understood [9,10]. A long-standing conjecture is that group locomotion provides hydrodynamic benefits as members move within the flows generated by others [5,9,11–13]. Assessing this hypothesis is challenging because the hydrodynamics of unsteady swimming at high Reynolds numbers is complex [14,15] and flow interactions among multiple swimmers yet more complex [9,16]. Early progress came from the calculations of Weihs indicating that each fish within a planar or two-dimensional group optimally exploits flows by swimming between the wakes left by two upstream neighbors, which themselves are positioned side by side [5,13]. The benefits extend to all members if the school assumes a crystalline arrangement with a diamond-shaped unit cell. Field and laboratory studies, on the other hand, have reported variable arrangements [6,8,17,18], leading some to emphasize social over hydrodynamic benefits [6,10,19,20]. However, fish display hydrodynamic exploitation by modifying swimming motions and reducing muscular effort in vortex-laden flows [7,9].

Some complexities of schooling can be addressed through mechanically actuated hydrofoils or airfoils, which have proven successful as analogs to fish swimming and flapping propulsion generally. Research aimed at the single locomotor level has found that flapping foils share with their biological counterparts many common aspects of the dynamics, flows, forces, and energetics [14–16,21]. An iconic similarity is the so-called reverse von Kármán wake left by fish and flapping foils [21–27]: An array of counter-rotating vortices surrounds a sinuous jetlike flow, as illustrated in Fig. 1(a). Experiments and simulations show that, so long as the Reynolds and Strouhal

^{*}jun@cims.nyu.edu

[†]ristroph@cims.nyu.edu

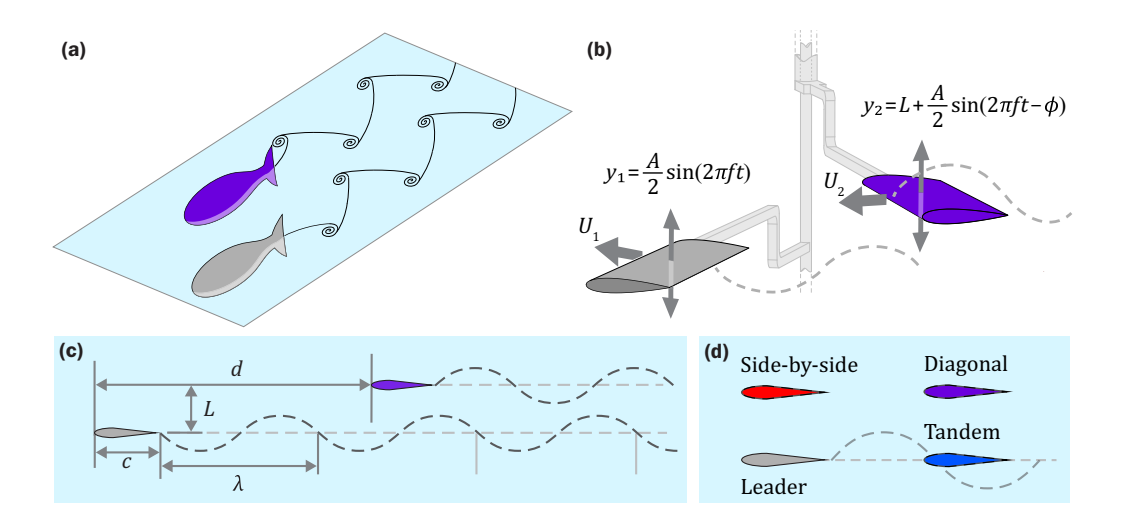


FIG. 1. (a) Sketch of two fish swimming in diagonal formation while interacting through vortex wakes. (b) Experiment consisting of two hydrofoils that are flapped up and down in a water tank (not shown), with each foil free to revolve about an axle. Flapping leads to forward propulsion, which takes the form of large orbits around the tank. (c) Definitions of the chord length c, lateral spacing L, streamwise displacement d, and trajectory wavelength λ . (d) For prescribed but variable lateral spacing, possible emergent formations include side-by-side (red), tandem (blue), and diagonal (purple) states.

numbers (defined below) are in the biologically relevant ranges, this wake structure is preserved for different body and propulsor shapes, for rigid and flexible propulsors, in two and three dimensions (2D and 3D), and for flapping kinematics including undulatory waveforms, pitching rotations, and heaving-and-plunging oscillations [14–16,21,25–33]. The hydrodynamic basis of schooling can be viewed as swimming while generating and interacting through such flows.

Recently, insights into schooling hydrodynamics have come from physical experiments and simulations aimed at multiswimmer interactions [32–39]. Tandem and freely interacting swimmers are observed to spontaneously assume one of several particular spacings [34,37,39], an observation that evokes a lattice or ordered formation. However, these previous studies confined foils to in-line positions and thus did not accommodate the side-by-side and diagonal formations that make up Weihs' model [5,13]. Here, we investigate the broader class of planar formations using a "robotic school" of self-propelling and hydrodynamically interacting flapping swimmers. By studying the two-body problem in which a "test fish" [purple in Fig. 1(a)] may take up any of in-line, side-by-side, or diagonal positions relative to a leader (gray), we map out the flow-mediated interactions and find that all such formations emerge spontaneously and are stabilized. This cohesion effect provides a hydrodynamic benefit that may assist in the formation and maintenance of schools and that operates across the diverse arrangements seen in nature [6,8,17,18].

Experimental approach. Our experiments employ hydrofoils with driven flapping motions that freely and interactively swim in water, with the locomotion of each foil in a pair coupled through the flows generated. To reproduce the quasi-2D situation of Fig. 1(a) in which the planes of interaction (streamwise-lateral) and motion (swimming-flapping) coincide, we construct the system represented schematically in Fig. 1(b). Each foil is mounted via a horizontal arm to a vertical axle that is driven to flap up and down by a motor. The axles are held by rotational bearings that allow each foil to move freely and independently in the azimuthal direction, and swimming takes the form of large rotational orbits within a water tank. Previous studies have shown good agreement between these experiments with rotational swimming and simulations of purely translational swimming for both isolated foils and pairs of interacting foils [25,35,37–41]. The swimming motions depend on the flapping

kinematics, which can be varied independently via motor controls, and the lateral spacing between the foils, which is systematically varied in order to explore tandem, side-by-side, and diagonal arrangements [Fig. 1(d)]. Additional details are given in the Supplemental Material [42], including evidence that wall effects and follower-to-leader interactions due to the rotational geometry are negligibly weak for the conditions studied here.

Compared to fish swimming, our approach idealizes the geometry and kinematics while employing parameter values that ensure the relevant fluid-dynamical regime and wake characteristics. The imposed flapping is pure heaving-and-plunging oscillations in which the vertical positions of the leader and follower foils are given by $y_1 = \frac{1}{2}A\sin(2\pi ft)$ and $y_2 = L + \frac{1}{2}A\sin(2\pi ft - \phi)$. Here, the prescribed lateral spacing is L = 0–10 cm, the peak-to-peak flapping amplitude A = 1–2 cm, frequency f = 2 Hz, and phase difference $\phi \in [0, 2\pi)$. Rigid foils of chord length c = 5 cm and span 15 cm are held at a distance 32 cm from the rotation axis to midspan. The spacing distance d between corresponding edges of the leader and follower [Fig. 1(c)] and the steady-state swimming speed d are measured outcomes that are observed to approach constant values as the foils match speeds and lock into formation. Importantly, the selected parameters yield amplitude-to-chord ratios d/c = 0.3–0.4, Reynolds numbers d0 Reynolds numbers d1 Reynolds numbers d2 Reynolds numbers d3 Reynolds numbers d4 Reynolds numbers d6 Reynolds numbers d6 Reynolds numbers d7 Reynolds numbers d8 Reynolds numbers d9 Reyn

Emergent formations and their stability. When initialized near one another, the foils swim forward and modify their relative position before matching speeds and falling into formation. The specific formation assumed depends on the flapping kinematics, the lateral spacing L between foils, and their initial streamwise separation d_0 . For example, the family of such arrangements achieved for fixed kinematics $(A = 2 \text{ cm}, f = 2 \text{ Hz}, \phi = \pi)$ and fixed lateral spacing (L/c = 1)but variable d_0 is shown in Fig. 2. When started within a body length ($|d_0| < c$), the foils align in the swimming direction with $d \approx 0$ and swim together in a side-by-side or abreast formation [gray-red pair in Fig. 2(a)]. Traces of the streamwise displacement d versus time t for several trials are shown as red curves in Fig. 2(b). The pair tightly locks into formation with only small deviations, suggesting strong stabilization. When started at greater separations ($|d_0| > c$), the foils fall into one of several diagonal formations [gray-purple pairs in Fig. 2(a)] that have discrete values of d. The corresponding traces shown as purple curves in Fig. 2(b) reveal a multiplicity of diagonal states separated by about one wavelength λ , which reflects the quasiperiodicity of the wake flow. Here, we include d > 0 and d < 0, and formations with the same |d| correspond to swapped roles for the leader and follower. Beyond $|d|/\lambda \approx 8$, no locked formations are observed and the swimmers drift in relative position rather than "school" together.

A close inspection of the traces in Fig. 2(b) reveals that more widely separated formations exhibit greater fluctuations in d and are less tightly locked. The positional fluctuations can be quantified through histograms of d, as shown in Fig. 2(c). This analysis uses the time-series data of Fig. 2(b) to determine the residence or occupancy time of different separations d across all formations. The sharply peaked distributions for more closely spaced formations imply strong interactions that tightly confine the group structure, while broader distributions for widely separated formations suggest a weakening of the cohesive fluid forces. Impressively, this locking effect is sufficiently strong to maintain formations even at distances as great as $d \approx 8\lambda$. Previous studies indicate that interfish spacings in schools are on the order of one body length [6,17,18], which corresponds to about 2λ given typical swimming characteristics [43], suggesting that fish are well within the range of hydrodynamic interactions.

Speed enhancement of side-by-side formations. These results indicate a multistability of formations, and indeed transitions between stable states are readily induced by applying external perturbations to the swimmers. In Fig. 2(d) we show the results of an experiment in which a follower initially in a diagonal state (d > 0) is impulsively "kicked" forward. It settles into the abreast position (d = 0) over about ten flapping cycles, and the pair thereafter remains locked side by side. Intriguingly, this transition is accompanied by a marked increase in speed for the pair. The

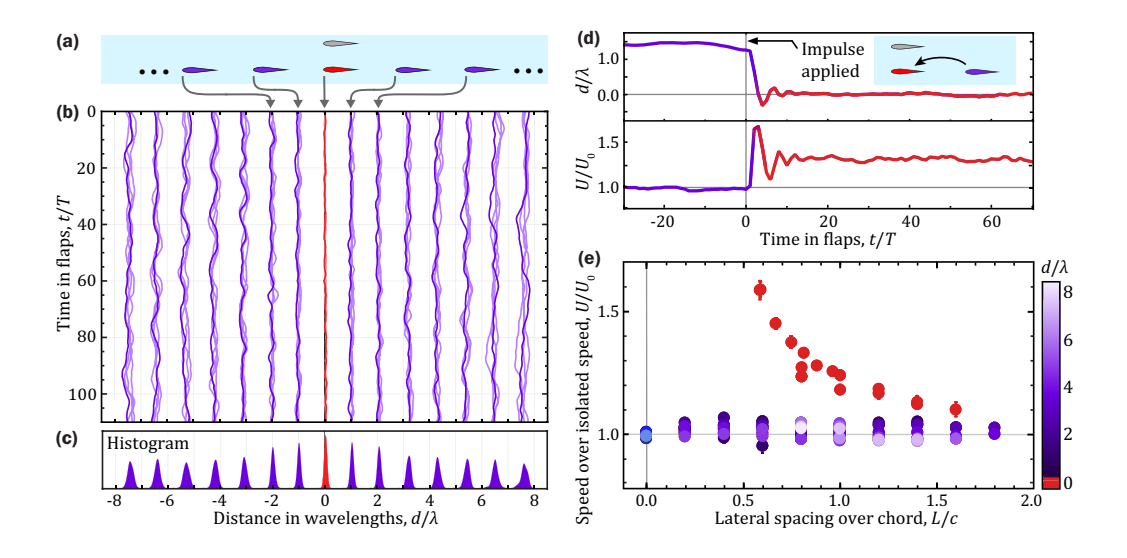


FIG. 2. (a) Multiple stable formations are observed in experiments of two swimmers with fixed lateral spacing and flapping kinematics. (b) Time series of streamwise separation distance normalized by wavelength d/λ . Side-by-side (red) and multiple, diagonal (purple) formations are attained by varying initial separation d_0 , and four trials are shown for each state. (c) A histogram of the distance between foils shows that more separated formations exhibit greater positional fluctuation. (d) An external impulse is applied to the follower in a diagonal formation at t=0, forcing a transition from diagonal (d>0) to side-by-side (d=0) formation. The side-by-side pair experiences an increase in swimming speed U. (e) Swimming speeds for formations with different lateral spacing L/c compared to the speed U_0 of an isolated foil.

lower panel of Fig. 2(d) displays the follower's speed over time, which matches the leader's in both formations, normalized by the measured speed U_0 of an isolated foil with the same flapping kinematics. The pair in a side-by-side formation travels about 30% faster than when the pair is in a diagonal formation, which has speed comparable to a solo swimmer.

To characterize the speed enhancement more generally, we measure the emergent speeds across side-by-side, diagonal, and tandem formations for A/c=0.3 or 0.4, f=2 Hz, and $\phi=\pi$. In Fig. 2(e) we compare all such states, which are distinguished by the streamwise and lateral separations, d and L. Tandem (d>0, L=0) and diagonal (d>0, L>0) pairs are represented by blue and purple circles and display speeds similar to that of an isolated foil. Side-by-side pairs (d=0, L>0), on the other hand, show significant speed enhancement, the strength of which depends on the lateral separation L [red circles of Fig. 2(e)]. The greatest boosts occur for closely spaced foils, and speeds up to 60% above that of a solo foil are attained for the conditions studied here.

Map of stable formations. We further seek a complete spatial map of locked formations across all values of (d, L) by systematically varying the lateral spacing L and initial streamwise spacing d_0 and measuring the stable gap distance (d-c) attained at later times. For example, the formations presented in Fig. 2 correspond to the solid diamonds in Fig. 3 along the horizontal line at L/c = 1. Varying L for the same kinematics $(A/c = 0.4, f = 2 \text{ Hz}, \phi = \pi)$ leads to the set of all solid diamonds. The stable states include tandem or in-line (blue), diagonal (purple), and side-by-side (red) positions for a follower relative to a leader (gray foil, not to scale). In Fig. 3 we report the stable gap distance over swimming wavelength $(d-c)/\lambda$ for each formation. This so-called schooling number proved useful in previous studies [35,37-39,44] as a dimensionless measure of the follower's location in the leader's wake flow, which is quasiperiodic with wavelength λ . Using this measure collapses the data for tandem and diagonal formations with different flapping kinematics,

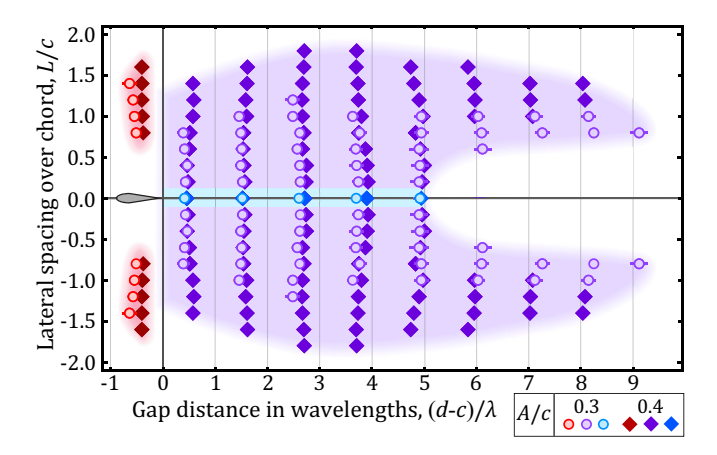


FIG. 3. Locking region for a follower relative to a leader. Spatial maps of stable formations across streamwise and lateral spacings (d, L) are shown for fixed flapping phase $\phi = \pi$ and two amplitudes A/c. The shaded regions show states accessible by changing the relative flapping phase ϕ .

as shown in Fig. 3 and previously studied for the tandem case [37,39]. Although not shown in Fig. 3, the equivalency of swapping the leader and follower implies a symmetry whereby the purple and blue data may be reflected to include d < 0.

Taken together, these results reveal a broad region in the vicinity of a given swimmer for which a second "test swimmer" may take up position and lock into formation. Surprisingly, the diagonal states of Fig. 3 extend significantly further downstream than tandem states. Thus, for a follower aiming to exploit the locking effect to keep pace with a leader, more states are available for laterally displaced positions. This property is robust to changes in flapping amplitude, as shown by the map formed by the open circles in Fig. 3 for the smaller value of A/c=0.3. While the locking region becomes more narrow for lower amplitude, it remains long ranged in the streamwise direction for diagonal configurations.

For a given A and L, it is observed that changing the relative temporal phase ϕ leads to shifts in d, as shown in Supplemental Fig. S2 [42]. Advancing ϕ through a complete cycle of 2π causes d to advance by λ , that is, $\Delta d \approx \lambda \Delta \phi/2\pi$. The vertical stripes in the data of Fig. 3 reflect the particular phase $\phi = \pi$, and other phase values lead to stable positions between these stripes. Thus the locking region is a true continuum as indicated by the background shading of Fig. 3. Further, the side-by-side state is observed for a range of phases $\phi/2\pi = 0.3$ –0.7 (Supplemental Figs. S2 and S3 [42]), indicating robust stability that does not require precise kinematic coordination between individuals.

Discussion. These results reveal the nature, range, and consequences of flow-mediated interactions between flapping hydrofoils. The broad variety of locked formations encompasses the tandem arrangements studied previously [34,37,39] and reveals many new states corresponding to side-by-side arrangements and a family of diagonal formations. Our results, along with theoretical studies [34,45–48], indicate that the swimmer interactions are not simply attracting or repelling but, quite generally across all formations, stabilizing. The interaction landscape seems to be highly corrugated, dotted with stable wells and valleys whose exact positions depend on the kinematics but whose great multiplicity lead to an effective region of stability. These findings highlight an intrinsic cohesiveness between group members that arises naturally from the flows generated during swimming.

The simplified system employed here is most analogous to fish swimming via caudal or tail fin oscillations and to highly aligned groups cruising at significant speeds. It remains for future work to test if hydrodynamic stabilization persists for the full complexity and variety of swimming modes used by schooling fish [14,15]. Encouragingly, for the tandem case specifically, similar interactions

have been observed for rigid and flexible swimmers, in 2D and 3D, across different kinematics, and in physical experiments, simulations, and mathematical models [34,35,37–39,45–48]. These similarities may be due to the robust generation of the reverse von Kármán wake by flapping swimmers [14–16,21,25–33].

Our results indicate that tandem and diagonal formations share a common stabilization mechanism involving specific phasing or coherence of a follower's flapping motions with the leader's quasiperiodic wake flow. Such interactions have been characterized in detail for tandem arrangements [34,37,39], and the key signatures of discrete spacings, their multiplicity, and wavelength and phase dependence are observed here across all diagonal positions. Because the locking region directly reflects the leader's wake in our experiments, the extended range of the diagonal over tandem formations can be interpreted as due to the lateral spreading of the wake, which is consistent with previous flow visualizations [35,37]. The side-by-side formations are not wake mediated, and their stability and speed-up are likely rooted in the so-called flapping ground effect that applies to a single swimmer adjacent to a wall as well as out-of-phase swimmers arranged in parallel [49–51]. These proposed mechanisms should be assessed and characterized through modeling and simulations.

Although our experiments are highly idealized compared to the collective locomotion of animals, some qualitative connections are intriguing. Notably, follower-wake phasing has been observed in recent studies of birds in formation flight [4] and fish swimming in pairs [52]. Specifically, ibises display pairwise phasing of wing-beat motions for staggered and in-line arrangements, and the follower in staggered pairs of goldfish shows a statistical preference for phase locking onto the leader's wake vortices. The latter is reminiscent of vortex slaloming behaviors displayed by other species of fish [7,9]. Further, side-by-side or phalanx formations have been shown to be preferentially adopted by collectively swimming fish when presented with sufficiently strong flows [53,54]. The positional stability and speed enhancement revealed here may be benefits of such configurations.

The passive stability emphasized here is but one factor contributing to the formation and maintenance of fish schools. The conventional hydrodynamic view emphasizes energy savings [5,9,11–13], which are not assessed in our experiments. However, recent simulations, models, and behavioral measurements show that such savings are available for a variety of relative positions [8,33,36,44,45]. Indeed, intrinsically stable formations may also be energetically efficient [46–48,55], consistent with swimmers working with, rather than against, intrinsic hydrodynamic effects. Passive mechanisms that assist in holding position, buffer collisions, and maintain group cohesion can save control effort and ease demands on sensorimotor systems [9,10,18,56]. Our findings suggest that such a hydrodynamic assist does not require highly specific positioning but rather operates across the diverse formations seen in nature [6,8,18]. For orderly and disorderly groups alike, it seems the intrinsic physical interactions promote staying in school.

Acknowledgments. We thank S. Ramananarivo, A. Oza, S. Childress, and M. Shelley for their comments. We acknowledge funding provided by New York University (NYU) Graduate School of Arts and Science (J.W.N.), an NYU Global Seed grant (L.R. and J.Z.), and an NSF Career grant (DMS-1847955 to L.R.).

J. Dunkel, S. Heidenreich, K. Drescher, H. H. Wensink, M. Bär, and R. E. Goldstein, Fluid Dynamics of Bacterial Turbulence, Phys. Rev. Lett. 110, 228102 (2013).

^[2] D. H. Kelley and N. T. Ouellette, Emergent dynamics of laboratory insect swarms, Sci. Rep. 3, 1073 (2013).

^[3] P. Lissaman and C. A. Shollenberger, Formation flight of birds, Science 168, 1003 (1970).

^[4] S. J. Portugal, T. Y. Hubel, J. Fritz, S. Heese, D. Trobe, B. Voelkl, S. Hailes, A. M. Wilson, and J. R. Usherwood, Upwash exploitation and downwash avoidance by flap phasing in ibis formation flight, Nature (London) 505, 399 (2014).

- [5] D. Weihs, Hydromechanics of fish schooling, Nature (London) 241, 290 (1973).
- [6] B. Partridge and T. Pitcher, Evidence against a hydrodynamic function for fish schools, Nature (London) **279**, 418 (1979).
- [7] J. C. Liao, D. N. Beal, G. V. Lauder, and M. S. Triantafyllou, Fish exploiting vortices decrease muscle activity, Science 302, 1566 (2003).
- [8] S. Marras, S. S. Killen, J. Lindström, D. J. McKenzie, J. F. Steffensen, and P. Domenici, Fish swimming in schools save energy regardless of their spatial position, Behav. Ecol. Sociobiol. 69, 219 (2015).
- [9] J. C. Liao, A review of fish swimming mechanics and behaviour in altered flows, Philos. Trans. R. Soc., B 362, 1973 (2007).
- [10] U. Lopez, J. Gautrais, I. D. Couzin, and G. Theraulaz, From behavioural analyses to models of collective motion in fish schools, Interface Focus 2, 693 (2012).
- [11] C. M. Breder, Vortices and fish schools, Zoologica 50, 97 (1965).
- [12] V. V. Belyayev and G. V. Zuyev, Hydrodynamic hypothesis of school formation in fishes, J. Ichthyol. 9, 578 (1969).
- [13] D. Weihs, Some hydrodynamical aspects of fish schooling, in *Swimming and Flying in Nature* (Springer, Berlin, 1975), pp. 703–718.
- [14] M. Sfakiotakis, D. M. Lane, and J. B. C. Davies, Review of fish swimming modes for aquatic locomotion, IEEE J. Ocean. Eng. 24, 237 (1999).
- [15] M. S. Triantafyllou, G. Triantafyllou, and D. Yue, Hydrodynamics of fishlike swimming, Annu. Rev. Fluid Mech. 32, 33 (2000).
- [16] M. S. Triantafyllou, A. H. Techet, and F. S. Hover, Review of experimental work in biomimetic foils, IEEE J. Ocean. Eng. 29, 585 (2004).
- [17] B. L. Partridge, T. Pitcher, J. M. Cullen, and J. Wilson, The three-dimensional structure of fish schools, Behav. Ecol. Sociobiol. 6, 277 (1980).
- [18] Y. Katz, K. Tunstrøm, C. C. Ioannou, C. Huepe, and I. D. Couzin, Inferring the structure and dynamics of interactions in schooling fish, Proc. Natl. Acad. Sci. USA 108, 18720 (2011).
- [19] B. L. Partridge, The structure and function of fish schools, Sci. Am. 246, 114 (1982).
- [20] J. K. Parrish and L. Edelstein-Keshet, Complexity, pattern, and evolutionary trade-offs in animal aggregation, Science 284, 99 (1999).
- [21] G. S. Triantafyllou, M. Triantafyllou, and M. Grosenbaugh, Optimal thrust development in oscillating foils with application to fish propulsion, J. Fluids Struct. 7, 205 (1993).
- [22] M. Lighthill, Hydromechanics of aquatic animal propulsion, Annu. Rev. Fluid Mech. 1, 413 (1969).
- [23] R. Blickhan, C. Krick, D. Zehren, W. Nachtigall, and T. Breithaupt, Generation of a vortex chain in the wake of a subundulatory swimmer, Naturwissenschaften 79, 220 (1992).
- [24] U. Müller, B. Van Den Heuvel, E. Stamhuis, and J. Videler, Fish foot prints: morphology and energetics of the wake behind a continuously swimming mullet (*Chelon labrosus* Risso), J. Exp. Biol. **200**, 2893 (1997).
- [25] N. Vandenberghe, J. Zhang, and S. Childress, Symmetry breaking leads to forward flapping flight, J. Fluid Mech. 506, 147 (2004).
- [26] J. H. Buchholz and A. J. Smits, The wake structure and thrust performance of a rigid low-aspect-ratio pitching panel, J. Fluid Mech. 603, 331 (2008).
- [27] A. Andersen, T. Bohr, T. Schnipper, and J. H. Walther, Wake structure and thrust generation of a flapping foil in two-dimensional flow, J. Fluid Mech. **812**, R4 (2017).
- [28] G. K. Taylor, R. L. Nudds, and A. L. Thomas, Flying and swimming animals cruise at a Strouhal number tuned for high power efficiency, Nature (London) 425, 707 (2003).
- [29] I. Borazjani and F. Sotiropoulos, Numerical investigation of the hydrodynamics of carangiform swimming in the transitional and inertial flow regimes, J. Exp. Biol. **211**, 1541 (2008).
- [30] I. Borazjani and F. Sotiropoulos, On the role of form and kinematics on the hydrodynamics of self-propelled body/caudal fin swimming, J. Exp. Biol. 213, 89 (2010).
- [31] D. Floryan, T. Van Buren, C. W. Rowley, and A. J. Smits, Scaling the propulsive performance of heaving and pitching foils, J. Fluid Mech. **822**, 386 (2017).

- [32] A. P. Maertens, A. Gao, and M. S. Triantafyllou, Optimal undulatory swimming for a single fish-like body and for a pair of interacting swimmers, J. Fluid Mech. 813, 301 (2017).
- [33] S. Verma, G. Novati, and P. Koumoutsakos, Efficient collective swimming by harnessing vortices through deep reinforcement learning, Proc. Natl. Acad. Sci. USA 115, 5849 (2018).
- [34] X. Zhu, G. He, and X. Zhang, Flow-Mediated Interactions between Two Self-Propelled Flapping Filaments in Tandem Configuration, Phys. Rev. Lett. 113, 238105 (2014).
- [35] A. D. Becker, H. Masoud, J. W. Newbolt, M. Shelley, and L. Ristroph, Hydrodynamic schooling of flapping swimmers, Nat. Commun. 6, 8514 (2015).
- [36] C. Hemelrijk, D. Reid, H. Hildenbrandt, and J. Padding, The increased efficiency of fish swimming in a school, Fish Fish. 16, 511 (2015).
- [37] S. Ramananarivo, F. Fang, A. Oza, J. Zhang, and L. Ristroph, Flow interactions lead to orderly formations of flapping wings in forward flight, Phys. Rev. Fluids 1, 071201(R) (2016).
- [38] S. Im, S. G. Park, Y. Cho, and H. J. Sung, Schooling behavior of rigid and flexible heaving airfoils, Int. J. Heat Fluid Flow 69, 224 (2018).
- [39] J. W. Newbolt, J. Zhang, and L. Ristroph, Flow interactions between uncoordinated flapping swimmers give rise to group cohesion, Proc. Natl. Acad. Sci. 116, 2419 (2019).
- [40] S. Alben and M. Shelley, Coherent locomotion as an attracting state for a free flapping body, Proc. Natl. Acad. Sci. USA 102, 11163 (2005).
- [41] S. E. Spagnolie, L. Moret, M. J. Shelley, and J. Zhang, Surprising behaviors in flapping locomotion with passive pitching, Phys. Fluids 22, 041903 (2010).
- [42] See Supplemental Material at http://link.aps.org/supplemental/10.1103/PhysRevFluids.7.L061101 for a description of the experimental apparatus and procedures as well as figures displaying additional data.
- [43] R. Bainbridge, The speed of swimming of fish as related to size and to the frequency and amplitude of the tail beat, J. Exp. Biol. 35, 109 (1958).
- [44] A. U. Oza, L. Ristroph, and M. J. Shelley, Lattices of Hydrodynamically Interacting Flapping Swimmers, Phys. Rev. X 9, 041024 (2019).
- [45] D. Weihs and E. Farhi, Passive forces aiding coordinated groupings of swimming animals, Theor. Appl. Mech. Lett. 7, 276 (2017).
- [46] Z.-R. Peng, H. Huang, and X.-Y. Lu, Collective locomotion of two closely spaced self-propelled flapping plates, J. Fluid Mech. 849, 1068 (2018).
- [47] L. Dai, G. He, X. Zhang, and X. Zhang, Stable formations of self-propelled fish-like swimmers induced by hydrodynamic interactions, J. R. Soc., Interface 15, 20180490 (2018).
- [48] S. G. Park and H. J. Sung, Hydrodynamics of flexible fins propelled in tandem, diagonal, triangular and diamond configurations, J. Fluid Mech. 840, 154 (2018).
- [49] E. Kanso and P. Newton, Locomotory advantages to flapping out of phase, Exp. Mech. 50, 1367 (2010).
- [50] J. Molina and X. Zhang, Aerodynamics of a heaving airfoil in ground effect, AIAA J. 49, 1168 (2011).
- [51] P. A. Dewey, D. B. Quinn, B. M. Boschitsch, and A. J. Smits, Propulsive performance of unsteady tandem hydrofoils in a side-by-side configuration, Phys. Fluids **26**, 041903 (2014).
- [52] L. Li, M. Nagy, J. M. Graving, J. Bak-Coleman, G. Xie, and I. D. Couzin, Vortex phase matching as a strategy for schooling in robots and in fish, Nat. Commun. 11, 5408 (2020).
- [53] I. Ashraf, H. Bradshaw, T.-T. Ha, J. Halloy, R. Godoy-Diana, and B. Thiria, Simple phalanx pattern leads to energy saving in cohesive fish schooling, Proc. Natl. Acad. Sci. USA 114, 9599 (2017).
- [54] J. de Bie, C. Manes, and P. S. Kemp, Collective behaviour of fish in the presence and absence of flow, Anim. Behav. 167, 151 (2020).
- [55] A. C. H. Tsang and E. Kanso, Dipole interactions in doubly periodic domains, J. Nonlinear Sci. 23, 971 (2013).
- [56] B. L. Partridge and T. J. Pitcher, The sensory basis of fish schools: relative roles of lateral line and vision, J. Comp. Physiol. 135, 315 (1980).